

Article

Thermal Maturity of the Silurian “Hot” Shales and Correlation with the Present Geothermal Variations in West Lithuania, Baltic Basin

Saulius Šliaupa ^{1,*}, Jurga Lazauskienė ² and Rasa Šliaupienė ¹

¹ State Scientific Research Institute Nature Research Centre, Akademijos 2, 08412 Vilnius, Lithuania; rasa.sliaupiene@gamtc.lt

² Department of Geology and Mineralogy, Vilnius University, M.K. Čiurlionio 21/27, 03101 Vilnius, Lithuania; jurga.lazauskiene@chgf.vu.lt

* Correspondence: saulius.sliaupa@gamtc.lt

Abstract: The most organic-rich shales are defined in the Dobele Fm. of the Aeronian Stage of about 10 m thick in west Lithuania. This particular layer is documented in the whole Baltic Basin. Compatible shales are widely distributed in other basins referred to as similar Silurian “hot” shales. The average TOC was estimated at 6.67 wt.% (good and excellent source rock). The thermal maturity of shales was evaluated through organic geochemical techniques, including TOC determination, Rock–Eval pyrolysis, and organic petrography studies. The thermal maturity varies from $T_{\max} = 431$ °C and eq.VR_o = 0.65% (early oil) to $T_{\max} = 468$ °C and VR_o = 1.38% (locally up to 1.94%) (late oil and wet to dry gas generation). It is notable, most of the study area is confined to regional-scale West Lithuanian Geothermal Anomaly. Most of the geothermal features, both palaeo- and recent, recorded in lateral variation in thermal maturity of shales unravel persistence of heat flow. Locally, the Variscan tectonic activity was imprinted in thermal maturity of organic matter-rich shales (Žemaičių Naumiestis anomaly).

Keywords: Baltic Basin; Llandovery; “hot” shales; thermal maturity; geothermal anomaly; palaeo-hydrothermal activity; “hot” granites



Academic Editor: Thomas Gentzis

Received: 24 March 2025

Revised: 16 May 2025

Accepted: 16 May 2025

Published: 19 May 2025

Citation: Šliaupa, S.; Lazauskienė, J.; Šliaupienė, R. Thermal Maturity of the Silurian “Hot” Shales and Correlation with the Present Geothermal Variations in West Lithuania, Baltic Basin. *Minerals* **2025**, *15*, 539. <https://doi.org/10.3390/min15050539>

Copyright: © 2025 by the authors. Licensee MDPI, Basel, Switzerland. This article is an open access article distributed under the terms and conditions of the Creative Commons Attribution (CC BY) license (<https://creativecommons.org/licenses/by/4.0/>).

1. Introduction

In the course of their evolution, most of the old Phanerozoic sedimentary basins were affected by the temporal variations in the geothermal conditions, e.g., heat flow, phases of increased tectonic activity, often associated with hydrothermal fluid circulation, thermal blanketing, deep erosion of sedimentary deposits, etc. The temporal temperature variations are imprinted in the diagenetic history of the sedimentary rocks, including the Baltic Basin [1–3]. Assessing thermal maturity through a multi-proxy study is an efficient approach for reconstructing the protracted geothermal history of old Phanerozoic basins [4–7]. The pioneering study by [8] stressed the unstable heat flow throughout the Phanerozoic, which was imprinted in the thermal maturity of OM.

The Silurian organic matter-rich shales comprise the thickest source rock formation in the Baltic Basin [2,9,10]. The highest concentration of organic matter (OM) is observed in the Llandovery and Wenlock age shales. The total organic carbon (TOC) content varies in a wide range from 1% to 19% in west Lithuania [11–14]. The highest TOC value was reported from the Dobele Formation shales (Aeronian Stage of the Llandovery Series).

The Silurian organic-rich shales account for 80%–90% of the Palaeozoic sourced hydrocarbons (HC) in North Africa, Turkey, Syria, and Jordan [15,16]. Similar characteristics of the most-rich Silurian shales are reported from the Upper Yangtze Basin situated in South China [17–19]. The term “hot” shales was introduced by [20]. In the North African and Arabian regions, the age of “hot” shales is attributed to the Rhuddanian Stage [21], e.g., the age of this particular layer is slightly older than that in west Lithuania.

The thermal maturity of organic-rich shales is a paramount parameter not only for the assessment of the source rock potential, but also for the reconstruction of the paleotemperatures [22]. The pioneering studies of the thermal maturity of OM unravelled an unstable palaeo-geothermal gradient in the Baltic basin [8]. The palaeo-gradient was estimated to be generally higher than the present geothermal gradient. The high rate of gradient was interpreted as a specific geothermal feature of the Variscan orogenic event in Central Europe [23,24].

In this study, the thermal maturity of the Dobele and Jūrmala shales was employed to map the palaeo-temperature distribution in west Lithuania, situated in the deeply buried part of the Baltic Basin. The present study aims to investigate the paleo-geothermal activity recorded in the thermal maturity of the Silurian shales and to correlate these with the recent geothermal parameters. The present temperatures are well documented in west Lithuania owing to extensive oil exploration drilling.

The present-day heat flow ranges from 40 mW/m² to 94 mW/m² in west Lithuania [25,26]. The West Lithuanian Geothermal Anomaly (55 × 95 km, 4820 km²) is the most remarkable geothermal feature showing the highest heat flux recorded in the Eastern European Platforms. Furthermore, the highest heat flow of this regional scale anomaly was accounted to the radiogenic heat production of the Mesoproterozoic Žemaičių Naumiestis batholith documented in the crystalline basement in southwesternmost Lithuania [27]. The variations in thermal maturity of the Llandovery shales and correlation with present-day geothermal parameters were discussed in the paper. Because of high OM content in “hot” shales, these source rocks are most susceptible to local palaeo- and recent variations in the geothermal system.

2. Petroleum Play of the Baltic Basin

The Baltic Basin is a proven hydrocarbon (HC) system. The most complete stratigraphic section, comprising all the Phanerozoic periods, was documented in the Lithuanian part of the basin [28]. It points to the protracted burial history of the basin and the evolution of the HC system. In particular, the thermal maturity was strongly imprinted in the Palaeozoic shales accumulated in the basin [5].

The basin is flanked by the Fennoscandian Shield and Mazury-Belarus High (Figure 1). The Latvian Saddle links the Baltic Basin in the west and the Moscow Basin in the east [29]. The Teisseyre-Tornquist Zone (TTZ) punctuated the western boundary of the Baltic Basin. It is the longest pre-Alpine tectonic lineament in Europe. The transition zone between the East European Craton (EEC) and the Paleozoic Platform is still a matter of discussion despite numerous geophysical and deep drilling. The zone extends 2000 km from the Baltic Sea [30,31] to the Black Sea.

A number of small oil fields were discovered in the basin (Figure 1). The petroleum play of the Baltic Basin comprises the most important Cambrian sandstone reservoir (shown on the map) and low-potential upper Ordovician detrital limestones and Silurian reef-like limestones. The reservoirs alternate with organic-rich shales of the Cambrian, Ordovician, and Silurian age (source rocks).

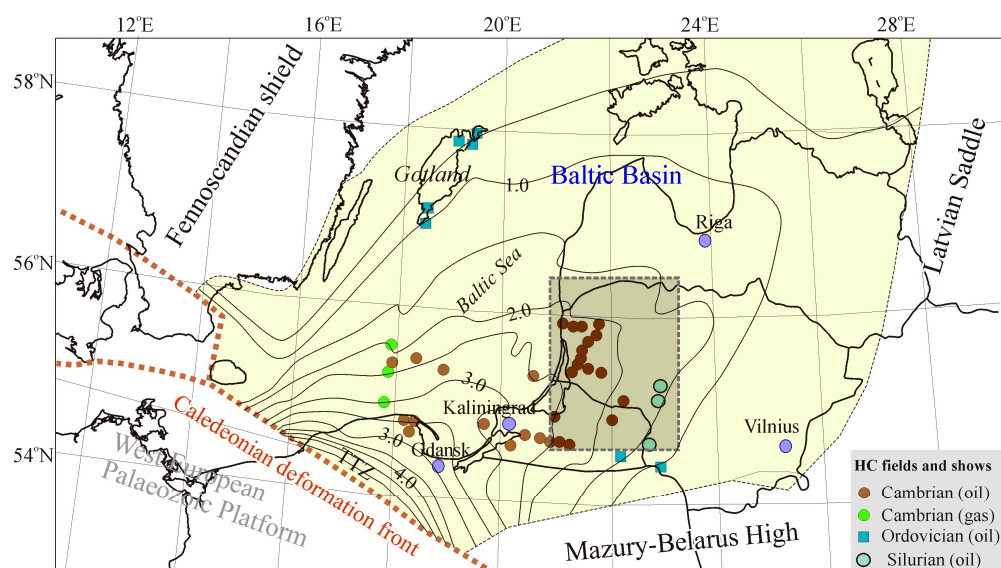


Figure 1. Baltic Basin and surrounding tectonic structures. The depth and distribution of the Cambrian reservoir (yellow). Oil fields are shown; colours indicate age of reservoir layers hosting oil fields; gas fields are indicated. Study area is indicated (Lithuanian part).

A number of small-sized oil fields onshore and offshore fields were discovered in the Cambrian sandstones in Lithuania, Kaliningrad District, and north Poland [12,32–34] (Figure 1). Also, several gas fields were discovered in the Polish sector of the Baltic Sea [35,36]. The depth of the top of the Cambrian reservoir varies from 1.7 to 3.3 km.

The Upper Ordovician carbonate mounds were exploited on Gotland Island [37] and oil accumulations (shows) were documented in the westernmost part of Latvia, middle Lithuania, and the eastern part of the Kaliningrad District. Notably, the oil migration pathways (oil smearing) are recognized in the easternmost periphery, extending as far as the Vilnius area [38]. It evidences long-distance migration of HC generated in deeply buried source rocks (Alum shales) and movement to the shallow basin periphery [39].

The not-exploited small oil fields were discovered in the upper Silurian bioherms and biostromes chained along the NNE-SSW trending belt in middle Lithuania [40–43]. These reef-like build-ups predominantly consist of stromatolites and crinoids. The sourcing HC to these stratigraphic traps is still a matter of discussion.

The hydrocarbons were generated from the Cambrian, Ordovician, and Silurian organic-rich shales. The biomarker tracing suggested the Alum Shale of the uppermost Cambrian and earliest Ordovician age as the main source rock for HC accumulated in the Cambrian, Ordovician, and Silurian reservoirs [39]. Also, the high concentration of the thermally mature upper Ordovician and lower Silurian shales is potentially accounted for by HC re-distribution in the Palaeozoic HC play [44,45].

The burial modelling suggested that the main HC generation phase was initiated in the Middle Devonian and climaxed in the Carboniferous time [46,47]. HC generation was fostered by increased geothermal activity associated with the Variscan igneous event. Numerous diabase sills were detected by extensive seismic surveys in the middle part of the present Baltic Sea and drilled by two exploration wells [48]. It is notable, both intrusions were emplaced in the Pridoli Series shales. The contemporaneous granite intrusion was drilled in well Girkaliai-2 in west Lithuania and cuts the Palaeoproterozoic crystalline basement [49].

Shales of the Llandovery and Wenlock Series comprise the most OM-enriched shales, while source rocks of the Ludlow and Pridoli Series show low concentration of OM (Figure 2) [13]. The thickness of the Llandovery and Wenlock shale package varies

from 113 m to 200 m in west Lithuania. The highest average TOC = 4.56% content of OM was recorded in the Dobele Formation (Fm.) of 2.5–10.5 m thick. The overlying shales are less enriched by OM (TOC = 1.45%) in the Jūrmala Fm. and Wenlock shales (Figure 2).

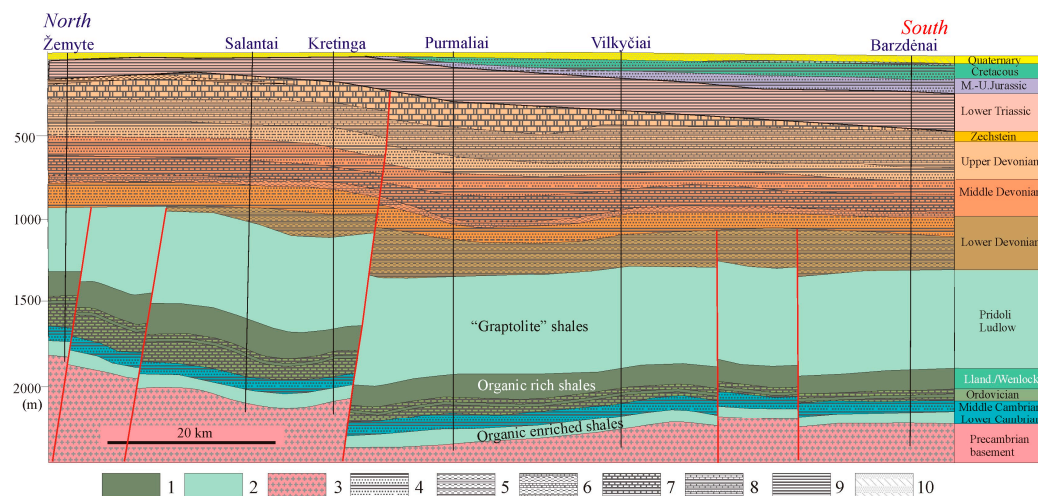


Figure 2. Geological N-S cross-section in westernmost Lithuania (see location of profile in Figure 5). Age of deposits is indicated. Most organic-rich shales are marked. Symbols: 1—“hot” shales, 2—organic-enriched shales, 3—crystalline basement, 4—sandstones with subordinate shales, 5—siltstones and limestones, 6—siltstones, claystones, dolomites, 7—limestones and dolomites, 8—marlstones and dolomites, 9—shales, 10—loam and sand.

The thickness of the upper part of the Silurian succession (Ludlow and Pridoli Series) is much larger, which was related to the progressing flexural bending of the Baltica plate during the latter part of the Silurian Period [41]. It resulted in a much lower concentration of OM in shales. The Ludlow mudstones show a low content of OM (0.45–1.0%) and decrease to <0.45% in the Pridoli shales. The detailed study of the mineral composition of the Llandovery Series was discussed in [13]. The content of clay minerals varies from 37% to 57%, and the amount of detrital quartz and feldspar ranges from 35% to 48%. The amount of the carbonates does not exceed 10%. Pyrite is a persistent diagenetic mineral recorded in the studied shales. Most of the studied shales are classified as silica-rich argillaceous mudstones.

The deepest, drilled in the sedimentary cover, well Klaipėda-1 (1981) illustrates the stratigraphic subdivision of the Llandovery and Wenlock Series. Figure 3 combines the interpretation of geophysical logging and was correlated with adjacent old wells drilled with continuous drill coring, including high-quality palaeontological recording (e.g., well Stoniškių-1) [50].

The very basal part of the Silurian succession is composed of micritic limestones that mark a new transgression of the marine basin, and this 2–4 m thick layer is referred to as the Stačiūnai Fm. devoid of graptolites (poor stratigraphic control) (Figure 3). Despite its low thickness, this layer is considered the key seismic reflector [43,51].

In general, most of the oil exploration wells were drilled with no coring and focused on the Cambrian interval drilled without coring. However, most of the wells have been drilled with coring in the lowermost part of the Silurian section (a few dozen meters long), consisting of fractured limestones of the Stačiūnai and Apaščia Fms. and overlying Dobele Fm. (most organic-rich shales) and Jūrmala Fm. (moderately enriched by OM shales). It provides abundant drill core material available for study.

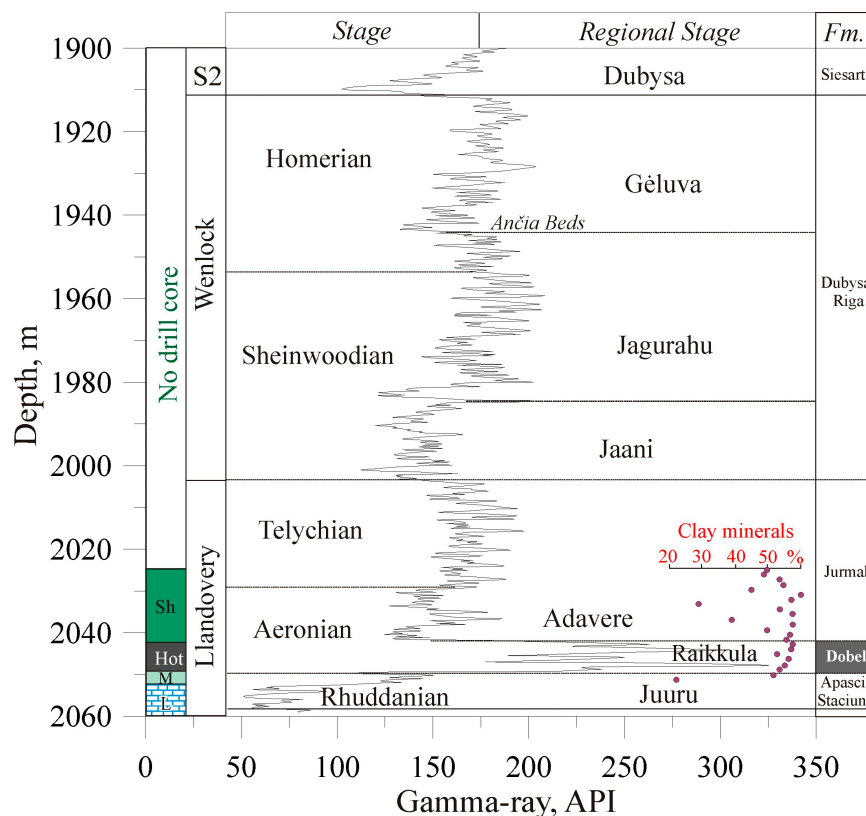


Figure 3. Gamma-ray log and drill coring interval in Llandovery and Wenlock Series in well Klaipėda-1 (see Figure 5 for location). Clay content is shown according to [13]. Symbols: Sh—organic enriched graptolitic shale, Hot—“hot” shale, M—marlstone, L—limestone.

The first graptolites are documented in the overlying 3–4 m thick Apaščia Fm. composed of mottled and wavy silty argillaceous limestones. This layer was referred to as the *Coronograptus cyphus* zone (depth 1921.0–1917.7 m defined in Figure 3, well Klaipėda-1) (Rhuddanian Series) and correlates with contemporaneous “hot” shales distributed in “southern” sedimentary basins.

The overlying “hot” shales are attributed to the Dobele Fm. of the Aeronian Series. Stratigraphy of this peculiar interval straddles: *Demirastrites triangulatus* zone defined at the depth of 1917.7–1915.0 m; *Demirastrites convalutus* zone at the depth of 1915.0–1912.2 m; and *Monograptus sedgawicki* zone at the depth of 1912.2–1909.9 m [50]. The Dobele Fm. represents the excellent stratigraphic marker correlating deep wells in Lithuania. The thickness of this peculiar layer ranges from 2.5 to 10.5 m in west Lithuania [13].

The gamma-ray characteristics are compatible with west Lithuanian and other Silurian well logs recording a strong ca. 350 API ‘spike’ marking the most organic matter-rich shales [52]. The lower gamma-ray values of about 170–180 API were reported in the Jūrmala Fm. and Wenlock Stage shales (Figure 3), which implies moderate enrichment in OM.

The Dobele Fm. shales are of dark grey and black, rarely olive grey colours and reveal variable bioturbation (Figure 4). The bioturbation records the transition of the anoxic (marked by the disappearance of bioturbation) to the suboxic sedimentation regime [53]. The burrows are distinguished by their brighter colour than the surrounding host rock in optical microscopy. Burrowing traces are ellipsoid (0.1–0.3 mm), oblique and horizontal to bedding, mainly restricted to particular laminae. Preferential calcite and dolomite cementation occurs in the burrow, promoting partial quartz and feldspar replacement. The observed

small burrow diameters are associated with low-oxygen stress [54]. Parallel-laminated shales contain thin interbeds and heterolith features.

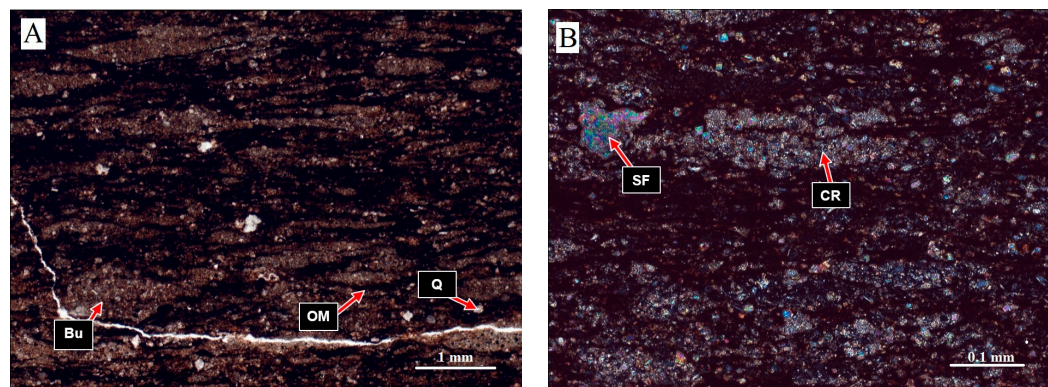


Figure 4. Micrograph of shales recording features at a scale of 1 mm (A) and 0.1 mm (B). Strongly bioturbated calcareous shale contains gently undulating, both discontinuous and continuous, parallel laminae. Abundant, c. 100–300 microns wide, elliptical, oblique to horizontal burrows are present throughout the sample. OM forms as elongate stringers and concentrations around burrows (Bu). Rare large carbonate skeletal debris is noted (SF). Microcrystalline to finely crystalline (Q), authigenic dolomite and calcite are preferentially concentrated within silt-filled burrows (SF). Middle Llandovery succession in well Žukai-1, west Lithuania, depth 1635.2 m.

The percentage of clay minerals varies from 37% to 57% in the Dobele and Jūrmala shales [13]. Clay minerals are dominated by illite with lower amounts of chlorite with subordinated admixture of mixed-layer illite-smectite (I-S) (5–10%) and kaolinite (2–7%). The content of quartz and feldspar grains is 11–40% and 2–10%, respectively. Early and late diagenetic micritic calcites are also recorded, and rare calcite shell fragments of 1–2 mm are documented. The euhedral late diagenetic crystals of dolomite are common in the studied shales. The total amount of carbonates does not exceed 5%, except for rare thin layers. Pyrite is recognized in varying amounts, and the siderite percentage is tenfold lower, though it is also recognized in all examined samples.

3. Materials and Methods

The lower Silurian shale samples were collected from 23 oil exploration wells drilled in the western part of Lithuania at a depth range from 1071 m (well Vilkaviškis-131) to 2134 m (well Pociai-1) (Figure 5). The data measured in this study were obtained from [55].

Rock-Eval analysis was performed on 257 Silurian shale samples studied and reported in (Table S1). Most of the samples were collected from Dobele Fm. ($N = 150$), Jūrmala Fm. ($N = 79$) and Wenlock Series ($N = 21$) (Table S1). Only 4 samples characterise the underlying Apaščia Fm. (basal part of the Silurian section), and 3 samples were obtained from shales of the Ludlow Series. The number of samples collected from the particular wells ranges from 1–2 (e.g., wells Akmenė-71, Malūkai-1, Mamiai-2) to 48 samples (well Geniai-1) and 58 samples (well Klaipėda-1, with the spacing at 0.5 m). Together with the previously reported laboratory measurements [45,56], the total number of studied samples amounts to 276 and were collected from 41 wells (Figure 5).

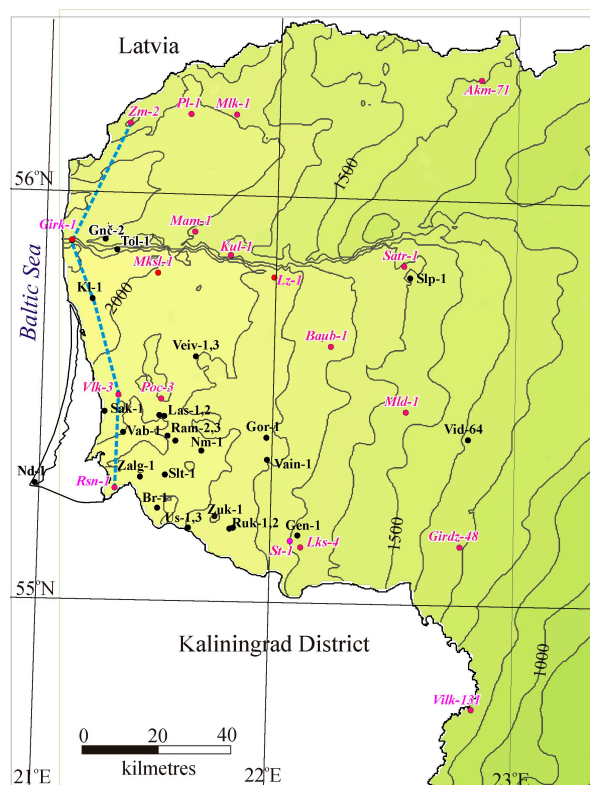


Figure 5. Map of the locations of the newly studied wells (black Normal) and previously studied wells (pink Italic) [45,55,56]. Abbreviations of well names: Akm-71—Akmenė-71, Baub-1—Baubliai-1, Br-1—Barzdėnai-1, Gen-1—Geniai-1, Girdz48—Girdžiai-48, Grk-1—Girkaliai-1, Gor-1—Gorainiai-1, Kl-1—Klaipėda-1, Kul-1—Kuliai-1, Las-1,2—Lašai-1, Lašai-2, Lks-4—Lauksargiai-4, Lz-Laužai, Mld-1—Malūkai-1, Mam-1—Mamiai-1, Nm-1—Žemaičių Naumiestis-1, Pl-1—Paluknė-1, Poc-3—Pociai-3, Ram-2,3—Ramučiai-2, Ramučiai-3, Ruk-1,2—Rukai-1, Rukai-2, Rsn-1—Rusnė-1, Sak-1—Sakučiai-1, Satr-1—Šatrija-1, Slt-1—Šilutė-1, Slp-1—Šlapgiriai-1, St-1—Stoniškiai, Tl-1—Toliai-1, Vab-1—Vabalai-1, Vain-1—Vainutas-1, Veiv-1,3—Veiviržėnai-1, Veiviržėnai-3, Vd-1—Viduklė-1, Vilk-131—Vilkaviškis-131, Vlk-3—Vilkyčiai-3, Us-1,3—Usėnai-1, Usėnai-3, Zlg-1—Žalgiriai-1, Zuk-1—Žukai-1. Depth isolines (b.s.l., m) of base of Silurian succession are shown. The geological cross-section (blue dashed line) extends along studied wells (Figure 2).

Rock-Eval pyrolysis parameters (TOC, T_{max} ; S1; S2; S3; HI; PI; OI) were derived from the Silurian shales (257 samples, Table S1). Rock-Eval pyrolysis and organic petrography were performed in world-class laboratories on the collected samples (e.g., Core Laboratories, Weatherford Laboratories). Measurements have been conducted using two methods. The organic substances were identified by combustion in a LECO IR212 induction furnace, after the elimination of carbonates, while Rock-Eval screening pyrolysis was carried out using the Rock-Eval II equipment, following the standardized guidelines outlined by [24,57] to assess the type of kerogen and the maturity of OM.

Open system pyrolysis was carried out with Rock-Eval 6 Analyser (standard model S/N 18-001) following the standard procedures described by [57,58] to assess the type of kerogen and thermal maturity of OM. Blank, standards, and duplicates were routinely run to ensure highly reliable results. The Rock-Eval 6 Analyser (standard model S/N 18-001) provides a rapid (30 min/sample) source rock analysis on a small (50–70 mg) sample of rock. All samples were powdered to a fraction below 0.2 mm. Each sample was heated at 300 °C for 3 min, followed by a programmed pyrolysis at 25 °C/min up to 650 °C under a helium flow. It was then oxidized at 600 °C for 7 min under an oxygen flow. The industry standard (IFP 160000) was used as a standard sample for calibration. This analysis quickly evaluates the concentration of volatile and soluble OM, plus the amount of pyrolysable OM

in the sample and thermal maturity. The S1 fraction (mg HC/g sample; mostly composed of small volatile molecules), in which the amount of HC released at 300 °C was measured. The peak S2 is the amount of HC released from the cracking of kerogen (mg HC/rock) and heavy HC during temperature-programmed pyrolysis (300–600 °C) and represents the existing potential of a rock to generate hydrocarbons. S3 represents the amount of CO₂ from breaking carboxyl groups and other oxygen-containing compounds in kerogen, obtained at 300–390 °C. The hydrogen index (HI) is the normalized S2 value (S2/TOC), expressed in mg HC/gTOC. The oxygen index (OI) is related to the amount of oxygen in kerogen and is the normalized S3 value (S3/TOC), expressed in mgCO₂/gTOC. The production index (PI) shows the level of thermal maturation [59].

The organic petrographic analysis of the organic matter was conducted on 155 selected samples collected from 16 wells (Table S1). The number of samples varies from 1 (Lašai-1, Žalgiriai-1) to 47 samples (Geniai-1) per well. The stratigraphic interval straddles the Apaščia (4 samples), Dobele (129 samples), and Jūrmala Fms. (79 samples) (Llandovery Stage), the Wenlock (21 samples), and Llandovery Stages (3 samples). Drill cores are stored in the Core Storage of the Earth Information Center, Lithuanian Geological Survey.

The sample preparation followed the conventional procedures, e.g., the core was cut perpendicular to the bedding, the core samples were embedded in a resin and polished in line with the procedure described in [60]. The reflectance measurements were performed in oil immersion samples following the standards of the laboratories. The organic petrographic analysis of random vitrinite-like particle reflectance measurements was performed. The reflectance of solid bitumen (BR_o), graptolite (GR_o), and chitinozoan (ChR_o) has been measured and these values were converted to equivalent vitrinite reflectance eq.VR_o (Tables S1–S3).

The solid bitumen and zooclasts have been analyzed in incident white and fluorescence light modes using a Zeiss Axio Scope microscope at 500x magnification. The OM reflectance was measured according to ASTM D7708 Standard [61]. The identification of the dispersed organic matter has been carried out following the TSOP/ICCP classification [62], and based on the ICCP 1994 System [63]. The identification of macerals was based on observations of their morphology, color, texture, and thermal maturity assessment of shales.

Graptolite reflectance was reported as eq.VR_o in (Table S1), amounting to 155 samples. Fifty to sixty measurements were performed on most samples. The measured reflectance of fragments of graptolites was not classified into granular and non-granular types of fossils. Based on optical observations, the latter type of graptolites dominated in shales. The standard deviation of recorded reflectance varies from 0.03 to 0.13. Graptolite reflectance (GR_o) was converted to equivalent vitrinite reflectance (eq.VR_o) by adopting the equation ($\text{Log}_{10} \text{GR}_o = -0.04 + 1.10 \times \text{Log}_{10} (\text{eq.VR}_o)$) [64].

The reflectance of chitinozoans was measured in eight wells (a total of 20 samples) (Table S2). Data were reported as ChR_o and eq.VR_o. The thermal maturity of chitinozoan reflectance (ChR_o) was converted to equivalent vitrinite reflectance by the equation ($\text{ChR}_o = 1.152 \times \text{VR}_o + 0.08$) [65].

Results of all studied samples demonstrate that the samples contain abundant amorphous matrix of bituminite. However, the reflectance was not systematically measured to reliably document the thermal maturity of the studied shales and has no importance for the interpretation of this study.

Solid bitumen was identified in large quantities in samples obtained from some wells located in southwesternmost Lithuania (e.g., Ramučiai-2, Rukai-2, Naumiestis-1, etc., Figure 5). The reflectance of solid bitumen was measured in eight wells (13 samples) and converted to equivalent vitrinite reflectance by adopting the equation ($\text{BR}_o = 0.618 \times \text{VR}_o + 0.4$) [66] (Table S3).

Several test samples were studied to define the thermal maturity of sporinite (two samples) and alginite (four samples) macerals.

The present temperatures were measured in most of the deep oil exploration wells in Baltic countries, including west Lithuania [26]. The temperature of the base of the Silurian succession was recorded in 149 wells.

4. Results

4.1. Organic Petrography

The microscopically identifiable organic matter was reported from studied shales containing graptolite, alginite, bituminite, solid bitumen, acritarch, sporinite, and liptodetrinites (Figure 6).

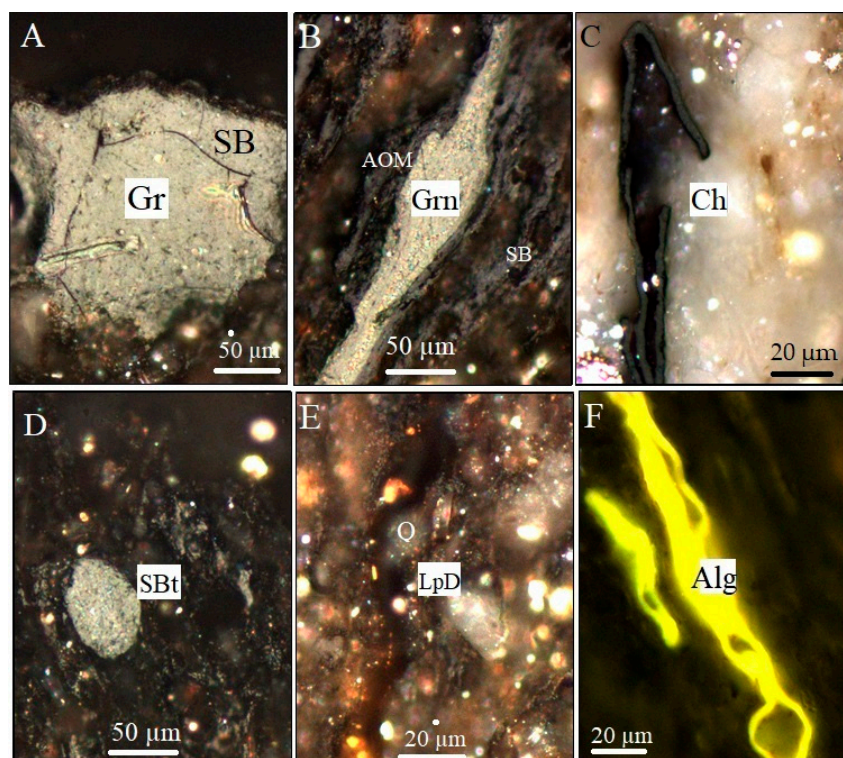


Figure 6. Organic petrography observations for Dobele Fm. shales: (A) graptolite (GR) is oriented perpendicular to bedding, shows traces of cortical bandage, incident light, VR_o -eq is 1.10%; graptolite shows traces of cortical bandage, incident light, Gorainiai-1, 1917.5 m; (B) granular graptolite (Grn), eq. VR_o was estimated 0.51%, network of wispy and elongate amorphous organic matter (AOM); solid bitumen (SB) is also present, some grains are spherical; incident light, well Viduklė-64, depth 1470 m; (C) broken fragment of chitinozoan (Ch), eq. VR_o was estimated 0.58%, Nida-1, 2044 m; (D) oval-shaped bitumen (SBt) with “rough surface”, eq. VR_o was estimated 1.05%, Gorainiai-1, 1917.5 m; (E) amber-coloured (mature) liptodetrinite (Type II, oil-prone) (LpD), abundant quartz grains (Q); incident light, Toliai-1, 1932.7 m; (F) marine alginite (Alg), most likely *Tasmanales*, intense yellow fluorescence colour (TAI = 2.7), Vidukle-64, 1470.0 m.

Graptolites are abundant in the lower Silurian shales accumulated in the deep shelf of the Baltic Basin. The reflectance of graptolites obtained from shale samples was converted to eq. VR_o % (Table S1). The reflectance of the Dobele Fm. varies from eq. VR_o % = 0.49% (Viduklė-64) to eq. VR_o % = 1.0% (Klaipėda-1).

The non-granular graptolites predominate in the studied samples (Figure 6A). Despite the mixture of non-granular and granular graptolites, the narrow standard deviation (0.03–0.011) points to the predominance of one type of graptolites. Scarce granular species are recognized in some samples (Figure 6B). No dedicated petrographic analysis was carried

out in the present study (granular vs. non-granular graptolites). The correlation between the reflectance of nongranular detritus and cortical bandages, recognized in some samples, reveals some difference in reflectance 0.82/0.92% (Usėnai-1, depth 1936 m), 1.01/1.19% (Gorainai-1, depth 1917.5 m), and 1.10/1.33% (Vabalai-1, depth 2010 m), test samples were not included into (Table S1).

The thermal maturity of chitinozoans was measured in reference wells (Figure 6C). The reflectance (not recalculated to equivalent vitrinite reflectance) varies from $ChR_o = 0.58\text{--}0.69\%$ (Nida-1, Geniai-1, Genčiai-1) to $ChR_o = 0.96\text{--}1.05\%$ (Klaipėda-1, Šilgaliai-1, Vainutas-1) (Table S2). The maximum reflectance was reported in the well Vainutas-1 ($ChR_o = 1.05$; converted to eq. $VR_o\% = 1.29$), which is compatible with high reflectance of graptolites (eq. $VR_o\% = 1.94$) [56]. This well is located in the Žemaičių Naumiestis anomaly and shows the highest thermal maturity of Llandovery shales.

The oil-prone bituminite is common in the studied Silurian shales. Bituminite occurs in the pores and coats mineral surfaces. Bituminite is generally characterized by higher intensity fluorescence and lower reflectance compared to solid bitumen.

Solid bitumen is often used to determine reflectance in samples with scarce other macerals [67]. Solid bitumen is present in the studied samples exclusively as solid bitumen of variable quality, comprised mostly of stringers and lenses. The reflectance of bitumen varies from $BR_o = 0.41\%$ (Nida-1) to $BR_o = 1.59\%$ (Ramučiai-1) (Table S3). The latter reflectance was converted to 1.81% (eq. VR_o) and reached the gas condensate stage. The illustration of the Gorainai-1 sample shows high thermal maturity (late oil generation stage) (Figure 6D; $BR_o = 1.05\%$).

Liptodetrinites (Type II, oil-prone) are observed in well Lithuanian shales (Figure 6E). Despite the wide occurrence of liptodetrinites, they have only limited importance in studying the thermal maturity of Silurian shales and were not used for thermal maturity studies.

Recent studies of the composition and maturation of the Silurian source rocks indicate a high content of dispersed sporinite [45]. The reflectance was recorded in a few test samples, indicating a very low reflectance 0.25% in well Šlapgiriai-1 (depth 1711 m) and 0.29–0.37% in the well Viduklė-64 (depth 1470 m) (Figure 6D) and was not used for mapping the thermal maturity of the studied shales.

Also, the thermal alteration index (TAI) was estimated in four test samples of alginite. UV fluorescent light color scale ranges from 2.7 (Viduklė-64, Figure 6F, yellow colour) to 3.1 (Vabalai-1, orange colour). The thermal maturity in the former well was rated as early to peak oil generation and late oil and gas generation stage in the latter wells situated in the Žemaičių Naumiestis anomaly. No systematic application of this technique was applied in the present study.

4.2. Rock-Eval Analysis

TOC is the primary parameter to evaluate the potential of HC generation. TOC value varies from 2.07% to 16.18% (average 7.29%) in 90% of samples of the Dobele Fm. shales. Some interlayers are poor in OM content (TOC = 0.31–1.99%) and subordinate argillaceous limestones. The enrichment in OM in the Jūrmala Fm. shales vary from 0.30% to 2.16% (average 1.14%) and 21 samples of the Wenlock Stage show similar values varying from 0.47% to 1.26% (average 1.17%). Three samples were obtained from Ludlow Stage shales and TOC varies from 0.34% to 0.46%. These results are compatible with those described in the introductory part of the manuscript (Figure 2).

The thermal evolutionary stages of kerogen and the heating of source rock layers are of paramount importance in evaluating the source rock potential [4,57,68]. The hydrogen index (HI) varies from 39 to 710 mg HC/g TOC (Table S1). The discrimination diagram by [69] ($(HI = S2(\text{mg/g})/\%TOC \times 100)$ vs. T_{max}) is commonly used to classify

the type of kerogen (Figure 7). Most studied samples are scattered in the transitional kerogen Type II/III zone, and shales, accordingly, are classified as oil-gas-prone source rocks. Notably, the gas-prone kerogen Type III was mapped in southwest Lithuania and is characterised by low HI in the Žemaičių Naumiestis anomaly (Figure 7). In general, most of the samples vary from T_{max} 430 °C to 450 °C, e.g., they are plotted in the oil window. Despite the wide scattering of values, T_{max} increasing with decreasing HI trend was noted.

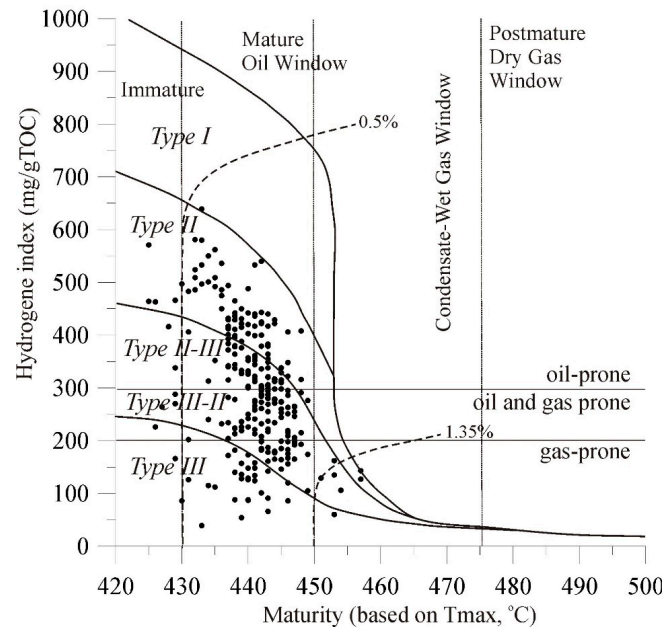


Figure 7. Plot of the hydrogen index (HI) vs. the pyrolysis maximum yield temperature (T_{max}) [69] of the Llandovery shales, showing the kerogen quality and thermal maturity stages.

A simple method for application in source rocks potential is based on Rock-Eval potential (S2) and TOC, w.%. The kerogen Type II shales are characterised by a relatively high HI (average HI is 480 mg HC/g TOC), while oil-gas-prone shales show a lower HI (259 mg HC/g TOC) (Figure 8). Gas-prone shales show the lowest HI values, ranging from 50 to <200 mg HC/g TOC).

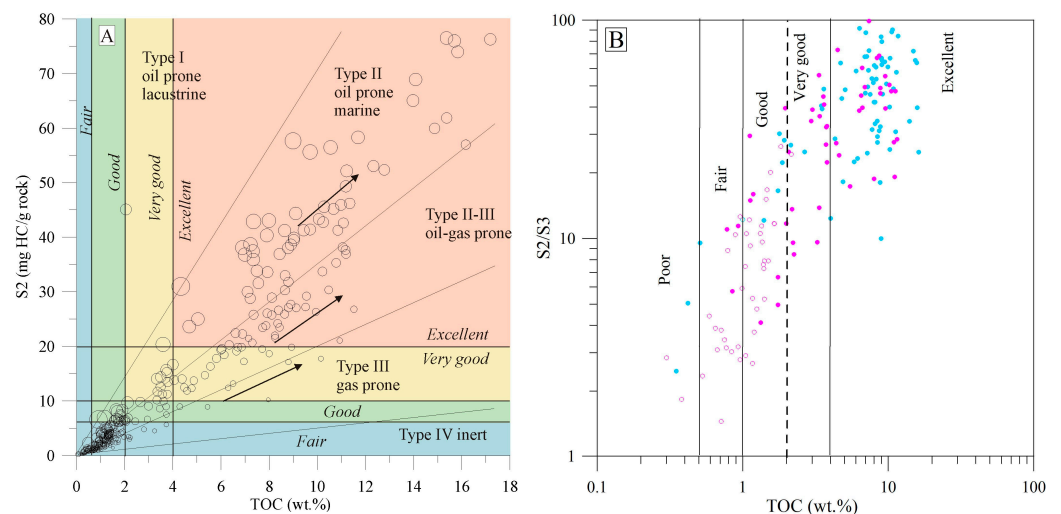


Figure 8. (A) Plot of TOC vs. S2 indicating the kerogen types of the studied Llandovery samples [70]; dot size shows increasing HI volume (min size 0.02 inch, max size 0.13 inch); trends are marked (arrows); (B) Cross-plot of TOC vs. Rock-Eval S2/S3 of Dobele Fm. (solid dots) and Jūrmala-Wenlock shales (open dots). General cluster of study samples is shown in blue, while samples collected from the Žemaičių Naumiestis anomaly are marked in pink (data derived from Table S1).

Types kerogen II, II/III, and III are identified on diagram TOC vs. S2 (Figure 8A). The organic richness of shales varies from fair to excellent (Figure 8A). In the high range of OM (TOC > 2.0 wt.%), the difference between the two trends of kerogen Type II and Type II/III is most spectacularly identified on the plot TOC vs. S2. A detailed inspection of the low-range interval (0.03 to 2.0 wt.%) shows less prominent discrimination of two clusters, which, however, are discernible on the plot. In particular, shales of the best-studied wells Klaipėda-1, Geniai-2, Šlapgiriai-1, Toliai-2, Vilkaiviškis-134 are chained along the Type II trend; the key wells Gorainai-1, Usėnai-1, and other boreholes are clustered in the Type II/III field (Figure 8A). The extreme values are scattered in the Type II (7–18%) while the Type II/III cluster shows much lower values (4–11%). Similar two trends were recognised in the plot TOC vs. S2/S3. The cluster kerogen Type III shows the lowest ratio as defined in the diagram TOC vs. S2 (Figure 8A). These wells Ž.Naumiestis-1, Usėnai-1, Šilutė-1, Ramučiai-1, Pociiai-1, Žatgiriai-1 are located in the Žemaičių Naumiestis anomaly. The studied shales are rated as ranging from fair to excellent source rocks (Figure 8B).

The ratio TOC vs. S2/S3 reflects the HC potential to generate oil and gas [4,71]. The average TOC was estimated as high as 6.67 wt.% (Table S1). Most of the shale samples (90%), collected from the Dobeles Fm., show good to excellent source rock quality for HC generation (Figure 8B; solid symbol). The overlaying shales of the Jūrmala Fm. (TOC = 1.10 wt.%) and Wenlock Series (TOC = 1.17 wt.%) are attributed to fair- and good-quality source rock [72]. As mentioned above (not studied in the present research), the content of OM is only 1.0–0.45 wt.% in the Ludlow and less than <0.45 wt.% in Pridoli shales (poor source rock).

The important difference was noted between Žemaičių Naumiestis anomaly shales and other samples in west Lithuania. The latter sample cluster shows a significantly lower S2/S3 ratio compared to the rest of the west Lithuanian shales (Figure 8B). The ratio was estimated at 26.3% and 38.1%, respectively. According to [73], the presence of secondary products typically leads to a decrease in T_{max} due to lower S2 values. It is discussed below concerning the thermal maturity defined by petrographic studies.

The kerogen type is defined by plotting the oxygen index (OI) vs hydrogen index (HI) on a Van Krevelen diagram (Figure 9A) for the studied source rock. The HI values show a wide range from 39 to 710 mg HC/g TOC (Table S1). Most of the bulk samples (94%) are attributed to the Type II and Type II/III kerogen (Figure 9A). The increasing thermal maturity with burial depth is noticed in the plot. Two sample families were discriminated, indicating “background” wells (blue symbol in Figure 9) and the wells situated Žemaičių Naumiestis anomaly (pink symbol). Statistically, there is no common trend recognised between OI vs. HI.

The samples plotted in the kerogen Type III field show a low HI and a distinct increase in OI values from 23 to 67 mgCO₂/g TOC, while the minimum HI is typical of a high thermal grade. Most of the samples attributed to Type III kerogen represent the Žemaičių Naumiestis anomaly (blue symbol in Figure 9). Based on the petrographic studies, Type III was seemingly not derived from the terrestrial plant matter. The other mechanism should be considered, e.g., secondary HC products generated at higher temperatures. It is imperative to note that ‘woody’ Type III OM does not exist in source rocks of Silurian age. Thus, Type III kerogen may represent poor preservation of algal material.

The S1/TOC ratio of 0.1–0.2 is an indicative feature of source rocks entering the window of oil maturation. The ratios exceeding >1.5 (recorded in wells Vainutas-1, Geniai-1, and Usėnai-1) indicate the contribution of migrated oil to the system. The range of 0.1–0.5 for the analysed samples suggests a non-migrated nature for the occurring HC (Figure 9A). The closed vs. open HC systems should also be considered. Most of the studied shales are clustered in the field of oil expulsion and oil-saturated shale, while shales obtained from the wells located in the Žemaičių Naumiestis anomaly are classified as moderately

saturated shale. Several samples might be attributed to technical or other inconsistencies (statistical error).

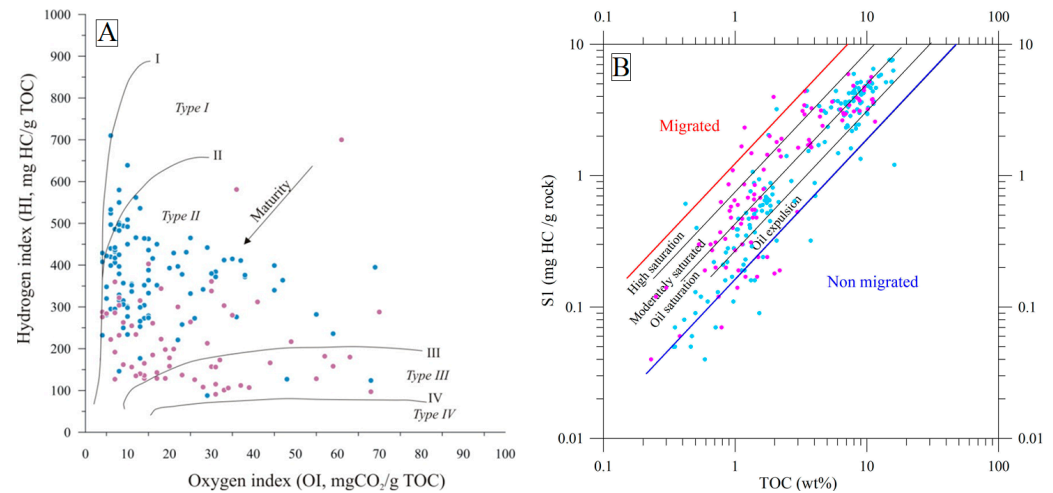


Figure 9. (A) Modified Van Krevelen diagram as OI vs. HI based on Rock-Eval pyrolysis showing hydrocarbon generative (kerogen) types in the studied Llandovery shales, west Lithuania; (B) Plot of TOC (wt.%) vs. Rock-Eval S1 (mg HC/g rock) of the Llandovery shales. General cluster of study samples is shown in blue, while samples collected from the Žemaičių Naumiestis anomaly are marked in pink (data derived from Table S1). Ranges are from [74].

5. Discussion

5.1. Control on Kerogen Type and Quality

The HC generation potential of the Llandovery and Wenlock Series is related to the high content of OM in graptolitic shales. As discussed above, the average enrichment in OM was assessed as high as 6.67% in the Dobeles Fm. (Aeronian) shales (thickness 2.5–10.5 m) and sharply decreases to 1.15% in the overlying Jūrmala Fm. (Aeronian and Telychian Stage) and Wenlock Series (total thickness 110–180 m). The Ludlow and Pridoli Series is characterised by poor HC-producing potential, with TOC is about c. 0.40%.

The thickness of the Silurian succession systematically increases to the west from 250 m to 870 m (Figure 10A). A peculiar gradient zone of about 100 m amplitude striking west Lithuania. This tectonic deformation seems to exert some the lateral pattern of kerogen types refined in the studied shales. Three kerogen trends were recognised on the plot TOC vs. S1 (Figure 8A), which correlate with three kerogen Type II, II/II, and III zones in the Llandovery shales (Figure 10B). The kerogen Type II zone is distributed in the shallow part of the study area and the kerogen Type II/III zone is defined in the deeper part of the basin. The transition between the two zones is marked by a sharp gradient in thickness (from 500 to 600 m) of the Silurian succession. The northern boundary is confined to the large Telšiai tectonic fault, and the eastern boundary is confined to the suspected Rambynas tectonic zone. The Telšiai Fault was nucleated in the latest Silurian time, and the most intense faulting took place in the earliest Devonian time, as based on seismic survey and well data [51] (Figure 10). The Rambynas Gradient Zone does not show any discernible faulting, as recorded in industrial profiles. The nature of this gradient zone is not well understood and is defined based on well data.

The kerogen Type III zone is a most peculiar feature recognised in the southwestern corner of Lithuania (Figure 10B). These shales are characterized by the lowest HI values and increased OI defined in six wells (Table S1).

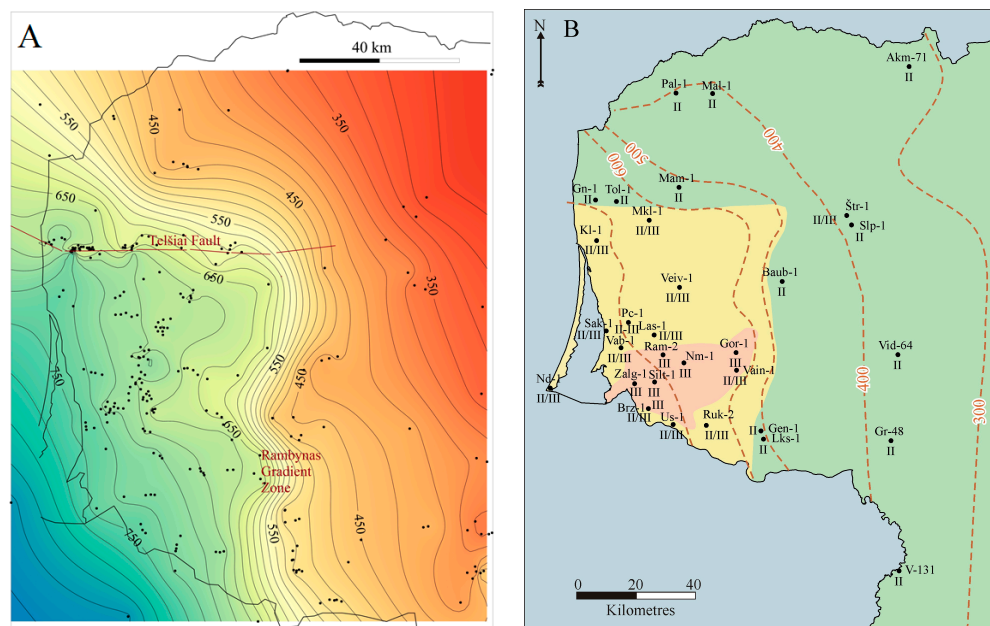


Figure 10. (A) thickness of the Silurian succession in west Lithuania. Wells penetrating the Silurian succession are indicated (black dots); Tešiai Fault and Rambynas Gradient Zone are indicated; (B) map of kerogen zonation (kerogen Types II, II/III, and III) recognised in Llandovery shales. The thickness of the Silurian succession is shown (brown contour line; m). Note that no “woody” organic matter (OM) existed in the Silurian shales, and the “Type III” nomenclature is, accordingly, reflecting oxidized OM.

The Production index “PI” is widely used in conjunction with other thermal maturity parameters [4,58]. In west Lithuania, PI ranges from 0.05 to 0.61 (combined present and previous study data), which indicates the oil window stage defined in all studied wells (Figure 11). Only well Malūlai-1 shows lower PI value (0.04). The highest PI values 0.26–0.61 are only partially confined to the Žemaičių Naumiestis anomaly and are attributed to the relatively high S2 and low S3 peaks. The latter is the characteristic feature of low HI range (Figure 9A). The studied samples show autochthonous kerogen type (Figure 9A), and no migration of hydrocarbons from source rocks interlayers can be suggested.

5.2. Thermal Maturity

A reflectance (R_o) and pyrolysis T_{max} temperature integrated contribute to assessing thermal maturity of shales and their lateral and temporal variations in the sedimentary basin [75], and the thermal maturity of the lower Silurian “hot” shales in particular [76]. Most of the study area is situated in the oil window, limited by the $T_{max} = 430$ °C contour line (Figure 11). The burial depth of the Dobele Fm. varies from approximately 1071 (Vilkaviškis-134) m to 2134 m (Pociai-7). The early oil and peak oil zones are defined in west Lithuania (Figure 12). The latter zone covers all oil exploiting fields.

The highest thermal maturity $T_{max} = 450$ – 680 °C was defined in the southwestern corner of Lithuania and these shales are classified as the peak oil/gas condensate generation stage. The maximum value of 468 °C was documented in well Ž Naumiestis-1 (Table S1). The kerogen Type III was reported in this anomaly. Furthermore, the most mature shales are defined within the boundaries of the Žemaičių Naumiestis geothermal anomaly ($T_{max} = 450$ – 468 °C) and Klaipėda geothermal anomaly ($T_{max} = 450$ – 451 °C) (Table S1).

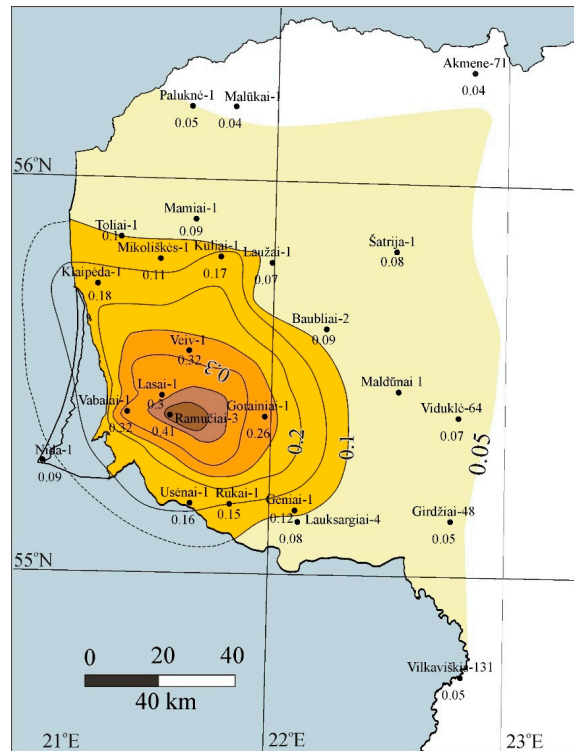


Figure 11. Production index (PI) trends of the Dobele Fm. shales of west Lithuania.

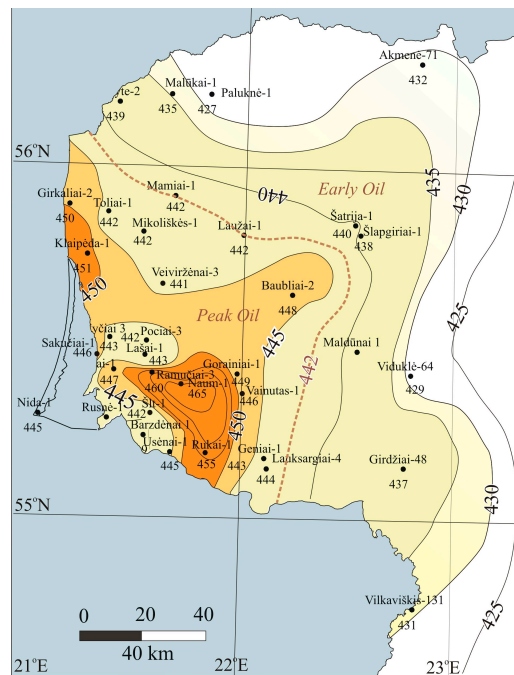


Figure 12. Rock-Eval T_{max} (°C) map of the lower Silurian shales. Studied wells and max T_{max} are shown. Early and peak oil zones are shown (boundary defined at 442 °C).

There are no definite limits of the West Lithuanian Geothermal Anomaly. The boundary of the anomaly is best discernible in the sharp increase in later diagenetic quartz cementation of the Cambrian sandstones [77]. It basically correlates with $T_{max} = 442$ °C isotherm and peak generation stage (Figure 13).

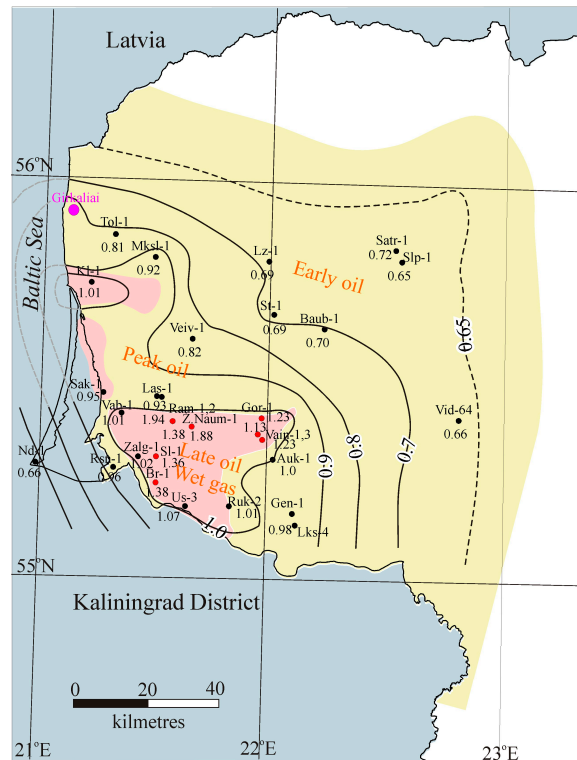


Figure 13. Thermal maturity map of the Dobele and Jūrmala Fms. shales succession based on vitrinite reflectance data (maximum eq. $VR_o\%$) (maximum reflectance defined in the well). Wells with anomalous reflectance values are highlighted in red. Pink polygons show the distribution of the Mesoproterozoic “hot” granitoids in Žemaičių Naumiestis, Traubai, Pilsotas areas (see Figure 14).

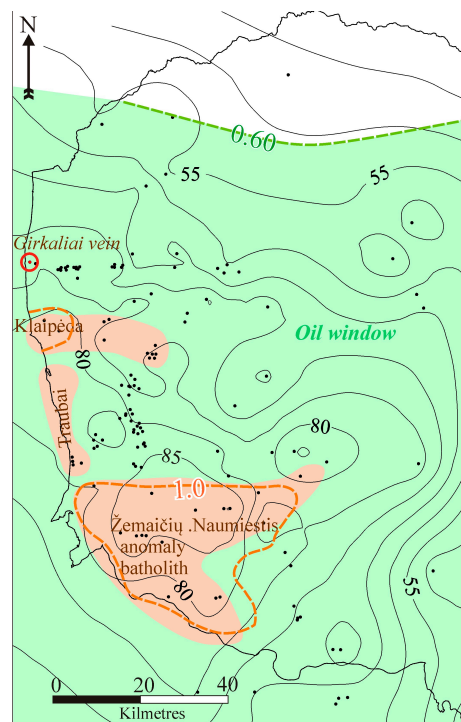


Figure 14. Present temperatures ($^{\circ}C$) distribution at the base of the Silurian succession in west Lithuania. Boreholes reaching the base of the Silurian are shown (black dots) (geothermal database of Lithuanian Geological Survey). Hatchet lines (green) mark eq. $VR_o = 0.60\%$ and (brown) eq. $VR_o = 1.0\%$. Brown polygons show distribution of the Mesoproterozoic “hot” granite (most of wells were drilled to the crystalline basement; [27,59]). Girkaliai granite vein (dated 355 Ma) is indicated by red circle [49].

The western limit of the West Lithuanian Geothermal Anomaly is controlled by only a few deep wells, e.g., old key well Nida-1 drilled in the Curonian Spit and offshore well D5-1 located 20 km west of Juodkrantė Village situated in the northern part of the Spit. Both wells show ca. 70 °C temperature at defined at the top of the Cambrian reservoir. The depth of the top Cambrian reservoir was defined at 2116 m in Nida-1 and 2332 m in D5-1. The depth of the top of the Wenlock Series was drilled at the depth of 1990 m in Nida-1. It extrapolates ca. 65 °C temperature that well correlates with moderate thermal maturity of Llandovery shales ($T_{\max} = 444$ °C and eq.VR_o% = 0.66).

The compilation of the thermal maturity map was based on petrographic observations. The reflectance of the most abundant graptolites and scarce chitinozoan and solid bitumen was converted to equivalent vitrinite-like reflectance to unify lateral variations recognised in thermal maturity of OM. Thermal maturity (eq.VR_o% = 0.65–0.66) was reported from wells Viduklė-64 and Šlapgiriai-1 that limited the oil window in west Lithuania (Figure 14). The limit of the Žemaičių Naumiestis anomaly was delimited by the contour line eq.R_o > 1.0 value (Figure 14). The equivalent vitrinite reflectance varies from eq.VR_o = 1.0 to 1.38% and reaches 1.81–1.94% (wells Ramučiai-1,3), incorporating present and previous data by [45,56]. Thirteen wells were studied and situated in the anomaly. The TAI measurement of the test sample collected from well Vabalai-1 shows the high thermal maturity TAI = 3.1 (colour scale) and was rated as the gas generation stage.

The southwestward systematic increase in thermal maturity was distinct in both maps (Figures 13 and 14) and climaxed in the Žemaičių Naumiestis anomaly. All wells producing oil from Cambrian sandstones in western Lithuania are situated in the peak oil production zone defined in the lower Silurian shales (eq.VR_o% > 0.80%). Based on old data [50], the sourcing of HC from Silurian shales is quite ambiguous and should rather be correlated with another source (Alum shale?).

The previous hydrochemical analysis of formation water samples from the well Stoniškiiai-1 (Figure 5) shows the paramount influence on the underlying and overlying HC reservoirs. The formation water contains 55–61% of dissolved gas CH₄ in the major Cambrian sandstone reservoir and overlying Ordovician and lower Silurian shales, while only a miserable concentration of CH₄ of about 0.1% was measured in the upper Silurian succession and Devonian aquifers [50]. Furthermore, the formation water of the Cambrian reservoir contains the low concentration of dissolved nitrogen of 29.8%, while nitrogen (77.2–87.4%) dominates the gas composition of the formation water of the upper Silurian and Devonian deposits.

The observed wide scattering in thermal maturity values is not sufficient to define any systematic organic matter facies pattern in west Lithuania. The visual inspection of samples shows no regularity in the distribution of liptinite macerals in the shales. The Rock-Eval studies, however, indicate distinct clustering of kerogen Types II, II/III, and III (Figure 8). The boundary of kerogen type II and II/III is confined to the two tectonic zones that originated in the upper Silurian and correlate with the burial depth transition (Figure 11).

The Type III, most likely, resulted from the higher percentage of the solid bitumen as indicated by petrographic studies of shale samples. The secondary bitumen is common in oil and gas fields. The geochemical characteristics and genesis of solid bitumen are not well understood. Also, according to [73], the presence of secondary products typically leads to a decrease in T_{\max} due to lower S₂ values. On the other hand, the overprint of palaeo-hydrothermal fluid flows ascending along the fractured shales implies a reasonable explanation of this phenomenon [71] and marks thermal maturity anomalies defined in southwest Lithuanian wells (Figure 14).

The high variation from $T_{\max} = 439\text{ }^{\circ}\text{C}$ to $468\text{ }^{\circ}\text{C}$ was defined in the narrow depth interval 1943.4–1990.0 m and implies hydrothermal circulation along the particular fracture zone defined at the depth of 1979.5 m in well Ž.Naumiestis.

The peak temperatures implied by hydrothermal activity can be calculated based on optical petrographic studies, by adopting an Equation (1):

$$T_{\text{peak hydrothermal temperature}} = [\ln(\text{eq.VR}_0) + 1.19]/0.00782 \quad (1)$$

The peak equivalent vitrinite reflectance values of 1.0–1.94% imply palaeo-temperature ranges from $135\text{ }^{\circ}\text{C}$ to $236\text{ }^{\circ}\text{C}$ in the limits of the Žemaičių Naumiestis geothermal anomaly. Still, this equation does not take into account the second basic kinetic parameter, i.e., the duration of OM maturation in time. It should be noted that a short heating duration might overestimate temperatures.

Based on the isotope dating of diabase sills, a thermal event strongly affected the recent Baltic Sea area at c. 354 Ma [48] (Figure 14). Two diabase sills were drilled in offshore wells D1-1 and C8-1 (Kaliningrad sector of the Baltic Sea). Both intrusions of 25 m (depth of top 1700 m) and 6 m (depth of top 1977 m) thick were emplaced in the Pridoli graptolitic shales. The sill, cut by well C8-1, is confined to the large-scale west–east striking Kaliningrad fault, extending from the south Baltic Sea to west Kaliningrad region (130 km long). Based on seismic data and correlation with exploration key wells, the fault was established in the Variscan tectonic stage [78]. Furthermore, granite veins dissect the crystalline basement along the Telšiai Fault zone in west Lithuania [49], which might have served as conduits for the hot fluid fluxes. These estimated high palaeo-temperatures were reported in northeast Poland ($120\text{--}160\text{ }^{\circ}\text{C}$) and, most probably, have been related to the Carboniferous magmatic event within the Baltic basin that resets the isotopic composition of clay minerals (322–339 Ma) [2].

The recent pattern in the heat flow shows a systematic increase from 38 mW/m^2 in east Lithuania to $70\text{--}94\text{ mW/m}^2$ in the west [25]. Furthermore, the present temperature of the Silurian shales ranges from $45\text{ }^{\circ}\text{C}$ in north and middle Lithuania to $90\text{ }^{\circ}\text{C}$ in the central part of the West Lithuanian Geothermal anomaly (Figure 14). The geothermal data [26] was used to compile the map of temperature at the base of the Silurian succession.

Moreover, the recent temperatures show consistent correlation with the thermal maturity of the Llandovery Shales discussed in the paper (e.g., T_{\max} values vary from $431\text{ }^{\circ}\text{C}$ to $468\text{ }^{\circ}\text{C}$) (Figure 13). The thermal maturity shales, estimated based on petrographic studies, show the closest agreement of thermal maturity of shales with recent temperatures (Figure 14).

Three large Mesoproterozoic granitoid intrusions, emplaced in the Palaeoproterozoic granulites, were discovered owing to regional-scale gravity and magnetic field mapping and extensive drilling (Figure 14). Forty-five deep wells were drilled into the Mesoproterozoic granitoid intrusions [27].

It should be noted that the Žemaičių Naumiestis geothermal anomaly is spatially confined to the Mesoproterozoic “hot” granite batholith. The heat flow variations largely reflect the lithological mosaics of the Palaeo- and Mesoproterozoic crystalline basement rocks that closely correlate with variations in the heat generation. The Mesoproterozoic granitoides are mostly enriched by K, U, and Th radiogenic elements [79]. The size of the geothermal anomaly was estimated as large as $40 \times 40\text{ km}$.

The West Lithuanian Geothermal Anomaly is largely accounted for by abundant “hot” radiogenic intrusions. Furthermore, the highest thermal maturity of the Llandovery shales correlates with basement features owing for heat high heat generation. The Variscan tectonic activation was imprinted in local thermal maturity anomalies defined the Silurian

organic matter reach shales. On the other hand, most of the geothermal features, both palaeo- and recent, recorded in west Lithuania are characterised as rather persistent.

6. Conclusions

The most enriched shales are defined in the Dobele Fm. of the Aeronian Stage of 2.5 to 10.0 m thick in west Lithuania. This peculiar layer is distributed in the Baltic Basin and similar shales are widely distributed in other basins referred to as “hot” shales, attributed to the slightly older Rhudanian shales. The average TOC was estimated 6.67 wt.% and shales are classified as good and excellent source rocks. The content of OM in the overlying shales of the Jūrmala Fm. and Wenlock Series sharply declines to about 1.15 wt.% (fair type of source rocks). Therefore, the Dobele Fm. is considered the most important Silurian event recorded in deeply buried organic matter. The organic-lean shales are documented in the Ludlow and Pridoli Series (about 0.5 wt.%).

The Rock-Eval studies indicate distinct clustering of kerogen Types II, II/III, and III. The boundary of kerogen type II and II/III is confined to the two tectonic zones that originated in the Silurian. The type III zone is not related to organic facies variations and is characterised by the highest thermal maturity, showing the increase in OI and abundance of solid bitumen, which likely traces the Variscan thermal activity imprinted in organic-rich shales.

The thermal maturity of shales was evaluated using Rock–Eval pyrolysis and organic petrography (graptolites, chitinozoans, and solid bitumen) studies. The thermal maturity ranges from $T_{\max} = 431$ °C and eq.VR_o = 0.65% (early oil) to $T_{\max} = 468$ °C and VR_o = 1.38, locally up to 1.94% [56] (late oil and wet to dry gas generation) defined in the local Žemaičių Naumiestis anomaly.

It is notable, most of the study area is confined to regional-scale West Lithuanian Geothermal Anomaly. Most of the geothermal features, both palaeo- and recent, recorded in lateral variation in thermal maturity unravel a rather stable geothermal system. Locally, the Variscan tectonic activity was imprinted in thermal maturity anomalies (Žemaičių Naumiestis) defined the Silurian organic matter reach shales. Furthermore, the anomaly is underlain by the Mesoproterozoic “hot” granites defined in the crystalline basement.

Supplementary Materials: The following supporting information can be downloaded at: <https://www.mdpi.com/article/10.3390/min15050539/s1>, Table S1. The defined Rock-Eval Pyrolysis parameters (TOC, Tmax, S1, S2, S3, HI, OI, PI) and graptolite reflectance measurement values in the Silurian shales samples from west Lithuania (compiled after [55]) and graptolite reflectance measurement values converted to equivalent vitrinite reflectance values (eq.VR_o); Table S2. Chitinozoan reflectance measurement (ChR_o%) database of the Lower Silurian Llandovery shales and chitinozoan reflectance data converted after (eq.VR_o = 1.152 × BR_o + 0.08) after [65]; Table S3. Solid bitumen reflectance (BR_o) was measured for Lower Silurian shales and reflectance was converted by adopting the equation (BR_o = 0.618 × VR_o + 0.4) [66].

Author Contributions: Conceptualization, S.Š.; methodology, J.L. and S.Š.; formal analysis, S.Š. and J.L.; investigation, S.Š., J.L. and R.Š.; writing—original draft preparation, S.Š. and J.L.; writing—review and editing, R.Š.; visualization, S.Š. and R.Š.; supervision, R.Š. All authors have read and agreed to the published version of the manuscript.

Funding: This research received no external funding.

Institutional Review Board Statement: Code of Academic Ethics of Nature Research Centre Scientists and Researchers approved by Research Council of State Scientific Research Institute Nature Research Centre (Resolution of 27 January 2011) downloadable at <https://gamtostyrimai.lt/en/akademines-etikos-komisija/> (accessed on 15 May 2025). Code of academic ethics of Vilnius University (Resolution

of 21 October 2020) downloadable at https://www.vu.lt/site_files/Studies/Study_regulations/Code_of_academic_ethics_VU.pdf (accessed on 15 May 2025).

Data Availability Statement: Data is contained within the article or Supplementary Materials.

Acknowledgments: This study was supported by the open access to the research infrastructure of the State Scientific Research Institute Nature Research Centre under the Lithuanian open-access network initiative. Cordial gratitude is expressed to John Marshall for providing a unique opportunity for microscopic analysis in the Southampton Oceanographic Institute. We kindly thank three reviewers for their valuable comments which helped to structure and improve the manuscript.

Conflicts of Interest: The authors declare no conflicts of interest regarding the publication of this article.

References

1. Barker, C.E.; Pawlewicz, M.J. Calculation of Vitrinite Reflectance from Thermal Histories and Peak Temperature: A Comparison of Methods. In *Vitrinite Reflectance as a Maturity Parameter*; ACS Publications: Washington, DC, USA, 1994.
2. Kowalska, S.; Wójtowicz, A.; Hałas, S.; Wemmer, K.; Mikołajewski, Z. Thermal History of Lower Palaeozoic Rocks from the East European Platform Margin of Poland Based on K-Ar Age Dating and Illite-Smectite Palaeothermometry. In *Annales Societatis Geologorum Poloniae*; Polskie Towarzystwo Geologiczne: Kraków, Poland, 2019. [[CrossRef](#)]
3. Derkowski, A.; Środoń, J.; Goryl, M.; Marynowski, L.; Szczerba, M.; Mazur, S. Long-distance Fluid Migration Defines the Diagenetic History of Unique Ediacaran Sediments in the East European Craton. *Basin Res.* **2021**, *33*, 570–593. [[CrossRef](#)]
4. Peters, K.E.; Cassa, M.R. Applied Source Rock Geochemistry: Chapter 5: Part II. In *Essential Elements*; Hal Leonard Corporation: Milwaukee, WI, USA, 1994.
5. Schovsbo, N.H.; Moron, J.M.; Nielsen, A.T.; Nicolas, G.; Petersen, H.I.; Stouge, S. Thermal Maturity of Lower Palaeozoic Shales in North-West Europe—Calibration of Proxies. In Proceedings of the 74th EAGE Conference and Exhibition Incorporating EUROPEC 2012, Copenhagen, Denmark, 4–7 June 2012.
6. Misra, S.; Das, S.K.; Varma, A.K.; Mani, D.; Kalpana, M.S.; Ekblad, A.; Biswas, S. Multi-Proxy Approach on the Hydrocarbon Generation Perspective of Barjora Basin, India. *Mar. Pet. Geol.* **2020**, *112*, 104108. [[CrossRef](#)]
7. Spina, A.; Cirilli, S.; Sorci, A.; Schito, A.; Clayton, G.; Corrado, S.; Fernandes, P.; Galasso, F.; Montesi, G.; Pereira, Z.; et al. Assessing Thermal Maturity through a Multi-Proxy Approach: A Case Study from the Permian Faraghan Formation (Zagros Basin, Southwest Iran). *Geosciences* **2021**, *11*, 484. [[CrossRef](#)]
8. Majorowicz, J.A.; Marek, S.; Znosko, J. Palaeogeothermal Gradients by Vitrinite Reflectance Data and Their Relation to the Present Geothermal Gradient Patterns of the Polish Lowland. *Tectonophysics* **1984**, *103*, 141–156. [[CrossRef](#)]
9. Poprawa, P. Shale Gas Potential of the Lower Palaeozoic Complex in the Baltic and Lublin-Podlasie Basins (Poland). *Przegląd Geol.* **2010**, *58*, 226–249.
10. Jarzyna, J.A.; Bała, M.; Krakowska, P.I.; Puskarczyk, E.; Strzępowicz, A.; Wawrzyniak-Guz, K.; Więclaw, D.; Ziętek, J. Shale Gas in Poland. In *Advances in Natural Gas Emerging Technologies*; Al-Megren, H.A., Altamimi, R.H., Eds.; InTech: London, UK, 2017; ISBN 978-953-51-3433-6.
11. Kadūnienė, E. Organic Matter in Oil Source Rocks. In *Petroleum Geology of Lithuania and Southeastern Baltic*; Institute of Geology: Vilnius, Lithuania, 2001; pp. 96–119. ISBN 978-9986-615-23-1.
12. Zdanavičiūtė, O.; Sakalauskas, K. *Petroleum Geology of Lithuania and Southeastern Baltic*; Institute of Geology: Vilnius, Lithuania, 2001; ISBN 978-9986-615-23-1.
13. Šliaupa, S.; Lozovskis, S.; Lazauskienė, J.; Šliaupienė, R. Petrophysical and Mechanical Properties of the Lower Silurian Perspective Oil/Gas Shales of Lithuania. *J. Nat. Gas Sci. Eng.* **2020**, *79*, 103336. [[CrossRef](#)]
14. Cichon-Pupienis, A.; Littke, R.; Froidl, F.; Lazauskienė, J. Depositional History, Source Rock Quality and Thermal Maturity of Upper Ordovician—Lower Silurian Organic-Rich Sedimentary Rocks in the Central Part of the Baltic Basin (Lithuania). *Mar. Pet. Geol.* **2020**, *112*, 104083. [[CrossRef](#)]
15. Soua, M. Paleozoic Oil/Gas Shale Reservoirs in Southern Tunisia: An Overview. *J. Afr. Earth Sci.* **2014**, *100*, 450–492. [[CrossRef](#)]
16. Luening, S.; Shahin, Y.M.; Loydell, D.; Al-Rabi, H.T.; Masri, A.; Tarawneh, B.; Kolonic, S. Anatomy of a World-Class Source Rock: Distribution and Depositional Model of Silurian Organic-Rich Shales in Jordan and Implications for Hydrocarbon Potential. *Bulletin* **2005**, *89*, 1397–1427. [[CrossRef](#)]
17. Zaixing, J.; Ling, G.; Chao, L.; Yuan, W.; Min, L. Lithofacies and Sedimentary Characteristics of the Silurian Longmaxi Shale in the Southeastern Sichuan Basin, China. *J. Palaeogeogr.* **2013**, *2*, 238–251.
18. Wang, X.; Zhu, Y.; Lash, G.G.; Wang, Y. Multi-Proxy Analysis of Organic Matter Accumulation in the Upper Ordovician–Lower Silurian Black Shale on the Upper Yangtze Platform, South China. *Mar. Pet. Geol.* **2019**, *103*, 473–484. [[CrossRef](#)]

19. Jiang, S.; Peng, Y.; Gao, B.; Zhang, J.; Cai, D.; Xue, G.; Bao, S.; Xu, Z.; Tang, X.; Dahdah, N. Geology and Shale Gas Resource Potentials in the Sichuan Basin, China. *Energy Explor. Exploit.* **2016**, *34*, 689–710. [[CrossRef](#)]
20. Boote, D.R.D.; Clark-Lowes, D.D.; Traut, M.W. Palaeozoic Petroleum Systems of North Africa. *Geol. Soc. Lond. Spec. Publ.* **1998**, *132*, 7–68. [[CrossRef](#)]
21. Luening, S.; Craig, J.; Loydell, D.K.; Storch, P.; Fitches, B. Lower Silurian ‘hot Shales’ in North Africa and Arabia: Regional Distribution and Depositional Model. *Earth-Sci. Rev.* **2000**, *49*, 121–200. [[CrossRef](#)]
22. Welte, D.H.; Horsfield, B.; Baker, D.R. *Petroleum and Basin Evolution: Insights from Petroleum Geochemistry, Geology and Basin Modeling*; Springer: Berlin/Heidelberg, Germany, 1997; ISBN 978-3-540-61128-8.
23. Nehring-Lefeld, M.; Modliński, Z.; Swadowska, E. Thermal Evolution of the Ordovician in the Western Margin of the East-European Platform: CAI and Ro Data. *Geol. Q.* **1997**, *41*, 129–138.
24. Skret, U.; Fabianska, M.J. Geochemical Characteristics of Organic Matter in the Lower Palaeozoic Rocks of the Peribaltic Syncline (Poland). *Geochem. J.* **2009**, *43*, 343–369. [[CrossRef](#)]
25. Urban, G. Новые Определения Теплового Потока в Пределах Тепловой Аномалии Балтийской Синеклизы. *Proc. Est. Acad. Sci. Geol.* **1991**, *40*, 24–32. [[CrossRef](#)]
26. Zajacs, A.; Shogenova, A.; Shogenov, K.; Volkova, A.; Sliupa, S.; Sliapiene, R.; Jöeleht, A. Utilization of Geothermal Energy: New Possibilities for District Heating Networks in the Baltic States. *Renew. Energy* **2025**, *242*, 122375. [[CrossRef](#)]
27. Motuza, G. *The Precambrian Geology of Lithuania: An Integratory Study of the Platform Basement Structure and Evolution*; Regional Geology Reviews; Springer International Publishing: Cham, Switzerland, 2022; ISBN 978-3-030-96854-0.
28. Paškevičius, J. *The Geology of the Baltic States*; Geological Survey of Lithuania: Vilnius, Lithuania, 1997; ISBN 978-9986-623-20-5.
29. Nikishin, A.M.; Ziegler, P.A.; Stephenson, R.A.; Cloetingh, S.A.P.L.; Furne, A.V.; Fokin, P.A.; Ershov, A.V.; Bolotov, S.N.; Korotaev, M.V.; Alekseev, A.S.; et al. Late Precambrian to Triassic History of the East European Craton: Dynamics of Sedimentary Basin Evolution. *Tectonophysics* **1996**, *268*, 23–63. [[CrossRef](#)]
30. Pharaoh, T.C.; Winchester, J.A.; Verniers, J.; Lassen, A.; Seghedi, A. The Western Accretionary Margin of the East European Craton: An Overview. *Memoirs* **2006**, *32*, 291–311. [[CrossRef](#)]
31. Ponikowska, M.; Stovba, S.M.; Mazur, S.; Malinowski, M.; Krzywicz, P.; Nguyen, Q.; Hübscher, C. Crustal Structure and Tectonic Evolution of the Southern Baltic Sea Interpreted from Seismic, Gravity and Magnetic Data. *ESS Open Archive* **2023**. [[CrossRef](#)]
32. De Vos, W.; Hagen, F.; Tim, P.; Smith, N.; Vejbaek, O.; Verniers, J.; Nawrocki, J.; Poprawa, P.; Belka, Z. Pre-Devonian, Petroleum Geological Atlas of the Southern Permian Basin Area. In *Petroleum Geological Atlas of the Southern Permian Basin Area*; EAGE Publications: Dubai, United Arab Emirates, 2010; pp. 58–69.
33. Pikulski, L.; Karnkowski, P.H.; Wolnowski, T. Petroleum Geology of the Polish Part of the Baltic Region—an Overview. *Geol. Q.* **2010**, *54*, 143–158.
34. Okhotnikova, E.S.; Yusupova, T.N.; Barskaya, E.E.; Ganeeva, Y.M.; Mukhametshin, R.Z. Geochemical Analysis of Crude Oils in Kaliningrad Oblast Oil Fields and Its Importance for Oil Production. *Pet. Chem.* **2021**, *61*, 994–1001. [[CrossRef](#)]
35. Domżałski, J.; Górecki, W.; Mazurek, A.; Myśko, A.; Strzetelski, W.; Szamałek, K. The Prospects for Petroleum Exploration in the Eastern Sector of Southern Baltic as Revealed by Sea Bottom Geochemical Survey Correlated with Seismic Data. *Przegląd Geol.* **2004**, *52*, 792–799.
36. Kotarba, M.J. Origin of Hydrocarbon Gases Accumulated in the Middle Cambrian Reservoirs of the Polish Part of the Baltic Region. *Geol. Q.* **2010**, *54*, 197–204.
37. Warwel, A.; Hübscher, C.; Hartge, M.; Artschwager, M.; Schäfer, W.; Preine, J.; Häcker, T.; Strehse, V.; Karušs, J.; Lüdmann, T. The Paleozoic Hydrocarbon System in the Gotland Basin (Central Baltic Sea) Leaks. *Earth Space Sci.* **2023**, *10*, e2023EA002883. [[CrossRef](#)]
38. Laškovas, J. *The Sedimentation Environments of the Ordovician Basin in the South-Western Margin of the East European Platform and Lithogenesis of Deposits*; Institute of Geology: Vilnius, Lithuania, 2000.
39. Yang, S.; Schulz, H.-M.; Schovsbo, N.H.; Bojesen-Koefoed, J.A. Oil–Source–Rock Correlation of the Lower Paleozoic Petroleum System in the Baltic Basin (Northern Europe). *Bulletin* **2017**, *101*, 1971–1993. [[CrossRef](#)]
40. Lapinskas, P. *Structure and Petroliferosity of the Silurian in Lithuania*; Institute of Geology: Vilnius, Lithuania, 2000.
41. Lazauskiene, J.; Sliupa, S.; Brazauskas, A.; Musteikis, P. Sequence Stratigraphy of the Baltic Silurian Succession: Tectonic Control on the Foreland Infill. *Geol. Soc. Lond. Spec. Publ.* **2003**, *208*, 95–115. [[CrossRef](#)]
42. Bičkauskas, G.; Molenaar, N. The Nature of the So-Called ‘Reefs’ in the Pridolian Carbonate System of the Silurian Baltic Basin. *Geologija* **2008**, *50*, 94–104. [[CrossRef](#)]
43. Kaminskas, D.; Michelevičius, D.; Blažauskas, N. New Evidence of an Early Pridoli Barrier Reef in the Southern Part of the Baltic Silurian Basin Based on Three-Dimensional Seismic Survey, Lithuania. *Estonian J. Earth Sci.* **2015**, *64*, 47. [[CrossRef](#)]
44. Zdanaviciute, O.; Bojesen-Koefoed, J.A. Geochemistry of Lithuanian oils and source rocks: A preliminary assessment. *J. Pet. Geol.* **1997**, *20*, 381–402. [[CrossRef](#)]
45. Zdanaviciute, O.; Lazauskiene, J. The Petroleum Potential of the Silurian Succession in Lithuania. *J. Pet. Geol.* **2007**, *30*, 325–337. [[CrossRef](#)]

46. Šliaupa, S.; Hoth, P. Geological Evolution and Resources of the Baltic Sea Area from the Precambrian to the Quaternary. In *The Baltic Sea Basin*; Harff, J., Björck, S., Hoth, P., Eds.; Central and Eastern European Development Studies (CEEDES); Springer: Berlin/Heidelberg, Germany, 2011; pp. 13–51. ISBN 978-3-642-17219-9.
47. Kosakowski, P.; Wróbel, M.; Poprawa, P. Hydrocarbon Generation and Expulsion Modelling of the Lower Paleozoic Source Rocks in the Polish Part of the Baltic Region. *Geol. Q.* **2010**, *54*, 241–256.
48. Motuza, G.; Šliaupa, S.; Timmerman, M.J. Geochemistry and ⁴⁰Ar/³⁹Ar Age of Early Carboniferous Dolerite Sills in the Southern Baltic Sea. *Est. J. Earth Sci.* **2015**, *64*, 233. [[CrossRef](#)]
49. Vejelyte, I.; Yi, K.; Cho, M.; Kim, N.; Lee, T. Intracratonic Carboniferous Granites in the Paleoproterozoic Crust of Lithuania: New SHRIMP U-Pb Zircon Ages. In *Goldschmidt Conference Abstracts*; Cambridge University Press: Cambridge, UK, 2011; p. 2079.
50. Kisnierius, J.L. *Key Well Stoniškiiai-1 in Lithuania*; Periodika: Vilnius, Lithuania, 1974; p. 201.
51. Grendaite, M.; Michelevičius, D.; Radzevičius, S. A Large Array of Inselbergs on a Continuation of the Sub-Cambrian Peneplain in the Baltic Basin: Evidence from Seismic Data, Western Lithuania. *Geol. Q.* **2022**, *66*, 1–14. [[CrossRef](#)]
52. Lüning, S.; Kolonic, S.; Loydell, D.K.; Craig, J. Reconstruction of the original organic richness in weathered Silurian shale outcrops (Murzuq and Kufra basins, southern Libya). *GeoArabia* **2003**, *8*, 299–308. [[CrossRef](#)]
53. Baucon, A.; Corradini, C.; Floris, M.; Briguglio, A.; Cabella, R.; Campomenosi, N.; Piazza, M.; Corrigan, M.G. Life in Near-Anoxic Conditions: A Case Study of the Ichnology and Infaunal Ecology of Silurian Graptolitic Black Shales from Sardinia, Italy. *Palaeogeogr. Palaeoclimatol. Palaeoecol.* **2020**, *556*, 109889. [[CrossRef](#)]
54. Gingras, M.K.; MacEachern, J.A.; Dashtgard, S.E. Process Ichnology and the Elucidation of Physico-Chemical Stress. *Sediment. Geol.* **2011**, *237*, 115–134. [[CrossRef](#)]
55. Lazauskienė, J. *Studies of the Geological Structure of the Early Palaeozoic Shaley Successions*; Lithuanian Geological Survey: Vilnius, Lithuania, 2015; pp. 51–56.
56. Zdanavičiūtė, O.; Lazauskienė, J. Organic Matter of Early Silurian Succession—the Potential Source of Unconventional Gas in the Baltic Basin (Lithuania). *Baltica* **2009**, *22*, 89–98.
57. Peters, K.E. Guidelines for Evaluating Petroleum Source Rock Using Programmed Pyrolysis. *AAPG Bull.* **1986**, *70*, 318–329.
58. Espitalie, J.; Deroo, G.; Marquis, F. La Pyrolyse Rock-Eval et Ses Applications. Deuxième Partie. *Rev. Inst. Fr. Pét.* **1985**, *40*, 755–784. [[CrossRef](#)]
59. Espitalié, J.; Laporte, J.L.; Madec, M.; Marquis, F.; Leplat, P.; Paulet, J.; Boutefeu, A. Méthode Rapide de Caractérisation Des Roches Mères, de Leur Potentiel Pétrolier et de Leur Degré d'évolution. *Rev. Inst. Fr. Pét.* **1977**, *32*, 23–42. [[CrossRef](#)]
60. Sachse, V.F.; Littke, R.; Jabour, H.; Schumann, T.; Kluth, O. Late Cretaceous (Late Turonian, Coniacian and Santonian) Petroleum Source Rocks as Part of an OAE, Tarfaya Basin, Morocco. *Mar. Pet. Geol.* **2012**, *29*, 35–49. [[CrossRef](#)]
61. *ASTM D7708*; Standard Test Method for Microscopical Determination of the Reflectance of Vitrinite Dispersed in Sedimentary Rocks. ASTM International: West Conshohocken, PA, USA, 2014.
62. Stasiuk, L.D. Status Report on TSOP-ICCP Dispersed Organic Matter Classification Working Group. *Soc. Org. Petrol. Newsl.* **2002**, *19*, 14.
63. Gonçalves, P.A.; Kus, J.; Hackley, P.C.; Borrego, A.G.; Hámor-Vidó, M.; Kalkreuth, W.; Mendonça Filho, J.G.; Petersen, H.I.; Pickel, W.; Reinhardt, M.J.; et al. The Petrology of Dispersed Organic Matter in Sedimentary Rocks: Review and Update. *Int. J. Coal Geol.* **2024**, *294*, 104604. [[CrossRef](#)]
64. Bertrand, R. Standardization of Solid Bitumen Reflectance to Vitrinite in Some Paleozoic Sequences of Canada. *Energy Sources* **1993**, *15*, 269–287. [[CrossRef](#)]
65. Goodarzi, F. Reflected Light Microscopy of Chitinozoan Fragments. *Mar. Pet. Geol.* **1985**, *2*, 72–78. [[CrossRef](#)]
66. Jacob, H. Disperse Solid Bitumens as an Indicator for Migration and Maturity in Prospecting for Oil and Gas. *Erdoel Kohle Erdgas Petrochem.* **1985**, *38*, 365–392.
67. Ulmishek, G. *Geologic Evolution and Petroleum Resources of the Baltic Basin: Chapter 31: Part II*; American Association of Petroleum Geologists: Tulsa, OK, USA, 1990.
68. Tissot, B.P.; Welte, D.H. *Petroleum Formation and Occurrence*; Springer Science & Business Media: Berlin/Heidelberg, Germany, 1984.
69. Mukhopadhyay, P.K.; Wade, J.A.; Kruege, M.A. Organic Facies and Maturation of Jurassic/Cretaceous Rocks, and Possible Oil-Source Rock Correlation Based on Pyrolysis of Asphaltenes, Scotian Basin, Canada. *Org. Geochem.* **1995**, *22*, 85–104. [[CrossRef](#)]
70. Passey, Q.R.; Creaney, S.; Kulla, J.B.; Moretti, F.J.; Stroud, J.D. A Practical Model for Organic Richness from Porosity and Resistivity Logs. *Bulletin* **1990**, *74*, 1777–1794. [[CrossRef](#)]
71. Seewald, J.S. Evidence for Metastable Equilibrium between Hydrocarbons under Hydrothermal Conditions. *Nature* **1994**, *370*, 285–287. [[CrossRef](#)]
72. Baskin, D.K. Atomic H/C Ratio of Kerogen as an Estimate of Thermal Maturity and Organic Matter Conversion. *AAPG Bull.* **1997**, *81*, 1437–1450. [[CrossRef](#)]
73. Yang, S.; Horsfield, B. Critical Review of the Uncertainty of Tmax in Revealing the Thermal Maturity of Organic Matter in Sedimentary Rocks. *Int. J. Coal Geol.* **2020**, *225*, 103500. [[CrossRef](#)]

74. Jin, H.; Sonnenberg, S.A. Source Rock Potential of the Bakken Shales in the Williston Basin, North Dakota and Montana. In Proceedings of the AAPG Annual Convention and Exhibition, Long Beach, CA, USA, 22–25 April 2012. [[CrossRef](#)]
75. Hunt, J.M. *Petroleum Geochemistry and Geology*, 2nd ed.; Freeman: New York, NY, USA, 1996; ISBN 978-0-7167-2441-4.
76. Albriki, K.; Wang, F.; Li, M.; El Zaroug, R.; Ali, A.; Samba, M.; Wiping, F.; Mohammed, R.S. Silurian Hot Shale Occurrence and Distribution, Organofacies, Thermal Maturation, and Petroleum Generation in Ghadames Basin, North Africa. *J. Afr. Earth Sci.* **2022**, *189*, 104497. [[CrossRef](#)]
77. Molenaar, N.; Cyziene, J.; Sliupa, S.; Craven, J. Lack of Inhibiting Effect of Oil Emplacement on Quartz Cementation: Evidence from Cambrian Reservoir Sandstones, Paleozoic Baltic Basin. *Geol. Soc. Am. Bull.* **2008**, *120*, 1280–1295. [[CrossRef](#)]
78. Stirpeika, A. *Tectonic Evolution of the Baltic Syncline and Local Structures in the South Baltic Region with Respect to Their Petroleum Potential*; Lithuanian Geological Survey: Vilnius, Lithuania, 1999; p. 175.
79. Sliupa, S.; Motuza, G.; Korabliova, L.; Motuza, V.; Zaludiene, G. Hot Granites of Southwest Western Lithuania: New Geothermal Prospects. *Tech. Poszuk. Geol.* **2005**, *44*, 26–34.

Disclaimer/Publisher’s Note: The statements, opinions and data contained in all publications are solely those of the individual author(s) and contributor(s) and not of MDPI and/or the editor(s). MDPI and/or the editor(s) disclaim responsibility for any injury to people or property resulting from any ideas, methods, instructions or products referred to in the content.